BIOCHEMISTRY
including biophysical chemistry & molecular biology

Article

pubs.acs.org/biochemistry

Quantification of Transthyretin Kinetic Stability in Human Plasma Using Subunit Exchange

Irit Rappley,[†,‡,§] Cecília Monteiro,[†,‡,§,⊥,#] Marta Novais,[⊥] Aleksandra Baranczak,[†,‡,§] Gregory Solis,[§,∥] R. Luke Wiseman,[§,∥] Stephen Helmke,[▽] Mathew S. Maurer,[▽] Teresa Coelho,[⊥,@] Evan T. Powers,[†] and Jeffery W. Kelly*[,†,‡,§]

[†]Department of Chemistry, [‡]The Skaggs Institute for Chemical Biology, [§]Department of Molecular and Experimental Medicine, and [∥]Department of Chemical Physiology, The Scripps Research Institute, La Jolla, California 92037, United States

[⊥]Unidade Clínica de Paramiloidose, [#]Department of Neurology, and [@]Department of Neurophysiology, Hospital de Santo António, 4099-001 Porto, Portugal

[▽]Department of Medicine and Clinical Cardiovascular Research, Columbia University, College of Physicians and Surgeons, New York, New York 10032, United States

Supporting Information

ABSTRACT: The transthyretin (TTR) amyloidoses are a group of degenerative diseases caused by TTR aggregation, requiring rate-limiting tetramer dissociation. Kinetic stabilization of TTR, by preferential binding of a drug to the native tetramer over the dissociative transition state, dramatically slows the progression of familial amyloid polyneuropathy. An established method for quantifying the kinetic stability of recombinant TTR tetramers in buffer is subunit exchange, in which tagged TTR homotetramers are added to untagged homotetramers at equal concentrations to measure the rate at which the subunits exchange. Herein, we report a subunit exchange method for quantifying the kinetic stability of endogenous TTR in human plasma. The subunit exchange reaction is initiated by the addition of a substoichiometric quantity of FLAG-tagged TTR homotetramers to endogenous TTR in plasma. Aliquots of the subunit exchange reaction, taken as a function of time, are then added to an excess of a fluorogenic small molecule, which immediately arrests further subunit exchange. After binding, the small molecule reacts with the TTR tetramers, rendering them fluorescent and detectable in human plasma after subsequent ion exchange chromatography. The ability to report on the extent of TTR kinetic stabilization resulting from treatment with oral tafamidis is important, especially for selection of the appropriate dose for patients carrying rare mutations. This method could also serve as a surrogate biomarker for the prediction of the clinical outcome. Subunit exchange was used to quantify the stabilization of WT TTR from senile systemic amyloidosis patients currently being treated with tafamidis (20 mg orally, once daily). TTR kinetic stability correlated with the tafamidis plasma concentration.

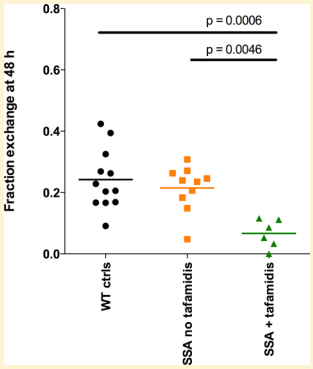

The amyloidoses are a group of degenerative diseases caused by the aggregation of a specific protein[1−7] leading to the dysfunction or loss of post-mitotic tissue.[8−11] Aggregation from an initially folded protein requires partial unfolding, exposing hydrophobic side chains and backbone H-bonding donors and acceptors that drive concentration-dependent aggregation.[12−15]

Transthyretin (TTR) is a tetrameric β-sheet-rich protein, secreted by the liver into the blood, wherein it transports holo-retinol binding protein and a small quantity of thyroxine.[16−18] The TTR tetramer concentration in human plasma varies from ≈3.4 to 5 μM.[19,20] Following rate-limiting tetramer dissociation and partial monomer denaturation, TTR can aggregate via a downhill polymerization mechanism to form fibrillar cross-β-sheet, or amyloid, deposits, as well as a spectrum of structurally diverse aggregates.[12,21−24] Dissociation of TTR tetramers begins by dimer separation along the weaker dimer−dimer interface comprising the thyroxine binding sites (Figure 1A).[25,26] Fast dimer dissociation to monomers, which can then misfold, leads to extracellular aggregation.[12,21,26−30]

Compelling human genetic and pharmacologic evidence supports the hypothesis that the process of TTR aggregation causes the degenerative phenotypes characteristic of the TTR amyloidoses.[9−11,23,31−36] Wild-type (WT) TTR aggregation causes senile systemic amyloidosis (SSA), primarily a cardiomyopathy occurring in ∼20% of the elderly population.[8] WT TTR aggregation on blood vessels also appears to play a central role in a variety of vascular diseases.[37] The autosomal dominant familial TTR amyloidoses present as a polyneuropathy [familial amyloid polyneuropathy (FAP)[38]] and/or a cardiomyopathy (familial amyloid cardiomyopathy[7,39]), depending on the identity of the *TTR* mutation the patient has inherited of the >100 disease-linked variants.[41,40]

Received: February 7, 2014
Revised: March 11, 2014
Published: March 12, 2014

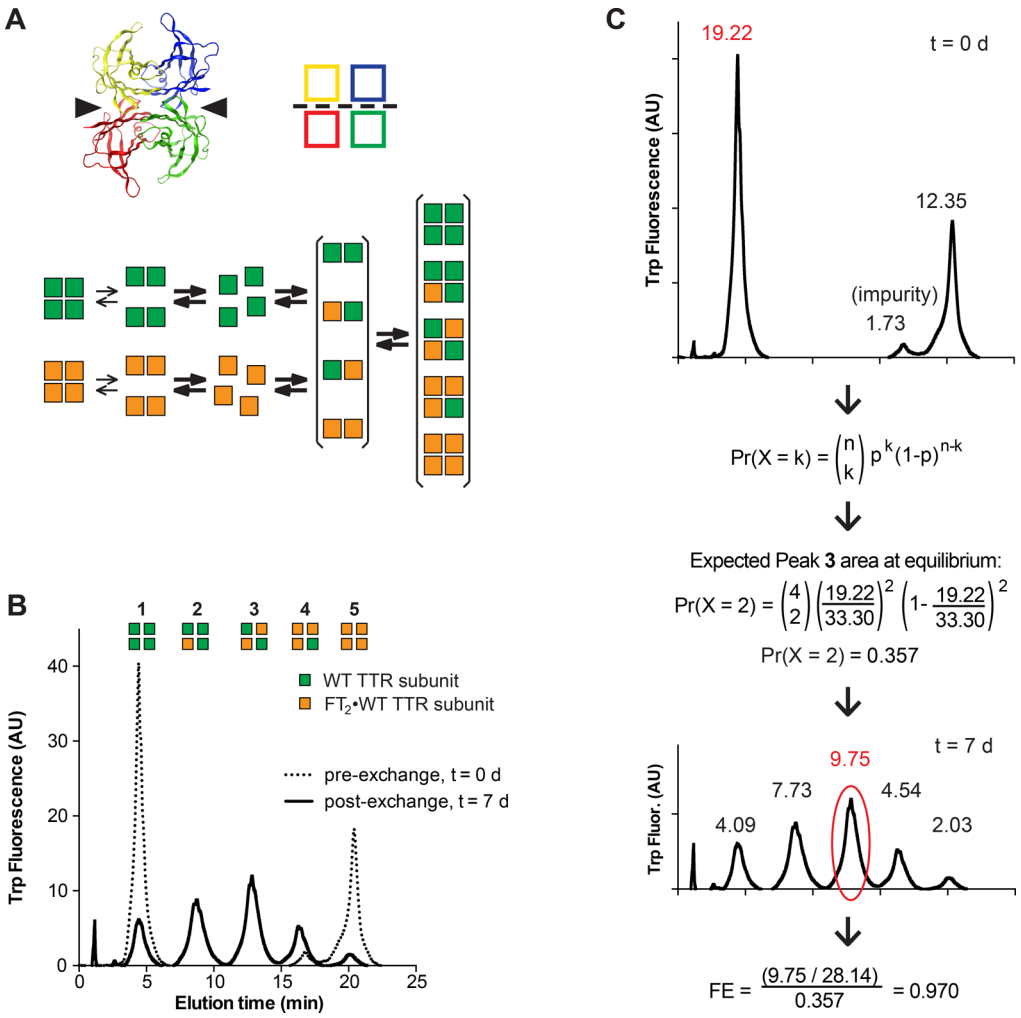

Figure 1. Subunit exchange measures the stability of recombinant TTR tetramers. (A) The top left panel shows a ribbon diagram of the TTR tetramer with individual subunits shown in different colors. Arrowheads indicate the thyroxine-binding pockets. The top right panel shows a cartoon of the same tetramer. The weak dimer−dimer interface is indicated with a dotted line. The bottom panel shows a schematic of the steps involved in dissociation, reassociation, and subunit exchange of untagged WT TTR subunits (green squares) and dual-FLAG-tagged (FT_2) WT TTR subunits (orange squares). (B) Recombinant WT and FT_2·WT TTR were mixed in equal amounts and separated by ion exchange chromatography after exchange for 7 days. The initial populations of homotetramers mix to create heterotetramers incorporating zero to four FT_2·WT TTR subunits. Green squares represent untagged WT TTR subunits and orange squares FT_2·WT TTR subunits. (C) To quantify subunit exchange, the relative area of peak **1** at time zero is calculated and used in the binomial equation to calculate the expected area of peak **3** at equilibrium. At each time point, the fraction exchange is calculated by comparing the actual relative area of peak **3** at that time point to the expected relative area of peak **3** at equilibrium (see the text for details).

The variability in the age of onset or the aggressiveness of the hereditary TTR amyloidoses can, in part, be attributed to differences in the thermodynamic and kinetic stability of heterotetramers comprising disease-associated and WT TTR subunits.[22,27,28,42−44] The decreased kinetic stability of TTR tetramers incorporating disease-associated subunits, i.e., their increased rate of dissociation, is correlated with their potential to cause pathology.[43] The therapeutic value of kinetic stabilization of TTR using small molecule drugs has been demonstrated in two placebo-controlled trials in heterozygous patient populations, wherein the TTR heterotetramers consist of a nearly statistical distribution of WT and destabilizing disease-associated mutant subunits.[9−11] In these trials, binding of the small molecule kinetic stabilizer drug tafamidis[9,10,31,45] or diflunisal[11,46−48] dramatically slows the progression of TTR polyneuropathy, as measured by neurologic impairment scores, quality of life assessments, and other metrics.[10,49] This provides strong evidence that the process of aggregation is the cause of these degenerative phenotypes. Furthermore, incorporation of T119M TTR subunits into tetramers otherwise composed of FAP-associated V30M TTR subunits kinetically stabilizes the heterotetramer, preventing the onset of FAP or resulting in very mild pathology.[22,23,34,35,50,51] T119M TTR subunit-associated kinetic stabilization of tetramers otherwise composed of WT TTR subunits also seems to prevent a range of vascular diseases, and the presence of T119M subunits extends human lifespan by 5−10 years.[37]

Because the decreased kinetic stability of the TTR tetramer is intimately linked to aggregation propensity and degenerative disease risk, a quantitative assessment of TTR kinetic stability in human plasma would serve as a biomarker for risk. This assay could also quantify a patient's response to kinetic stabilizer treatment, which is especially valuable for patients carrying substantially destabilized, rare, or currently uncharacterized TTR mutations. If the extent of small molecule-mediated stabilization of the TTR tetramer could be shown to correlate

dx.doi.org/10.1021/bi500171j | *Biochemistry* 2014, 53, 1993−2006

with clinical outcome in a future study, quantification of TTR kinetic stability could become a much-needed surrogate biomarker reasonably likely to predict clinical outcome in TTR amyloidosis patients.

Currently, the best available method for assessing TTR stability in human plasma calls for acid or urea denaturation of plasma, followed by glutaraldehyde cross-linking and SDS−PAGE separation of the plasma proteins. TTR immunoblotting can be employed to quantify the amount of tetramer remaining after denaturation as a function of time[31,47] (unfolded monomeric TTR is highly modified by glutaraldehyde treatment, precluding TTR antibody recognition of the monomer). Alternatively, immunoturbidity can be used to quantify the amount of TTR tetramer remaining after denaturation and cross-linking.[31] A limitation of these related methods is that they assess the stability of TTR under non-native conditions. Moreover, rigorous quantification of the electrophoresis gels is challenging.

Herein we report a simple, highly reproducible, alternative approach for quantifying the kinetic stability of TTR tetramers in human plasma based on the previously reported subunit exchange assay for quantification of the kinetic stability of recombinant TTR in buffer.[35,52−55] Importantly, this assay is conducted under physiological conditions, allowing for a TTR kinetic stability assessment directly in blood plasma, in the presence of all of the factors that could contribute to the stability of TTR and/or to the efficacy of small molecule TTR kinetic stabilization. Furthermore, this assay is inherently quantitative and reproducible and eliminates the difficult measurements for quantifying cross-linked TTR. For these reasons, we believe that the subunit exchange assay in human plasma could be useful in both academic and clinical settings to assess individual differences in the kinetic stability of endogenous TTR, to establish optimal dosing strategies for patients and to measure their response to treatment, and possibly as a biomarker for early diagnosis. We have already made several surprising observations about the kinetic stability of TTR in plasma using this assay, further highlighting the need for a quantitative *in situ* assay for TTR kinetic stability.

EXPERIMENTAL PROCEDURES

Expression and Purification of Recombinant TTR. Recombinant WT and dual-FLAG-tagged WT (FT_2·WT) TTR were expressed in and purified from *Escherichia coli* as described previously,[53] except that the buffer in the final gel filtration purification step consisted of 10 mM sodium phosphate (pH 7.6), 100 mM KCl, and 1 mM EDTA, hereafter termed "standard phosphate buffer". The molar absorbtivities (ε) of WT TTR (73800 M^{-1} cm^{-1}) and FT_2·WT TTR (85720 M^{-1} cm^{-1}) tetramers in standard phosphate buffer were used to calculate TTR concentrations.

Plasma Samples. Blood from healthy volunteers was obtained from The Scripps Research Institute's Normal Blood Donor Services Center. The blood was collected in BD Vacutainer tubes prepared with sodium citrate and allowed to sit upright for at least 30 min at room temperature. The blood was then centrifuged at 1500*g* for 20 min. The resulting supernatant (plasma) was carefully removed and centrifuged for an additional 20 min to remove any remaining cells. Aliquots of the clarified plasma were stored at −20 °C. Frozen plasma samples were thawed on ice before being used and then stored at 4 °C for up to 1 week. Plasma from TTR knockout (KO) mice was generously provided by J. Buxbaum of The Scripps Research Institute. Blood from SSA patients and WT controls was collected in 8 mL BD Vacutainer Cell Preparation Tubes (CPT) with Sodium Citrate/Ficoll, and after collection, each tube was stored upright at room temperature for 40 min. The blood was remixed immediately prior to centrifugation by gently inverting the tube 8−10 times and then centrifuged at room temperature (18−25 °C) in a horizontal rotor for 20 min at 1700*g*. After centrifugation, approximately one-half or one-third of the plasma was aspirated with a Pasteur pipet without disturbing the cell layer. Plasma was transferred to 1.5 mL cryovials with a cap and stored at −75 °C until it was shipped.

Subunit Exchange Studies with Recombinant TTR in Buffer. The indicated concentrations of untagged and dual-FLAG-tagged (FT_2) recombinant WT TTR tetramer in standard phosphate buffer were incubated at 25 °C, and the reaction was followed for up to 8 days. At each time point, a 50 μL sample, without or with an **A2** incubation step as described below, was injected onto a Waters Acquity H-Class Bio-UPLC (ultra performance liquid chromatography) instrument fitted with a strong anion exchange column. TTR was eluted from the column using a nonlinear gradient at a flow rate of 0.6 mL/min over 33 min (see the Supporting Information for additional details). Tryptophan fluorescence, with excitation at 295 nm and emission at 335 nm, was monitored at a sampling rate of one point per second. Where indicated, samples were incubated with 30 μM **A2** for 3 h before separation by ion exchange chromatography. **A2**-modified TTR conjugate fluorescence was monitored, using excitation at 328 nm with emission at 430 nm, at a sampling rate of one point per second. Peaks **1**−**5** were integrated using Empower 3 software according to the manufacturer's instructions.

Subunit Exchange Studies using Endogenous WT TTR in Human Plasma. Frozen plasma samples, collected as described above, were thawed on ice and stored as needed at 4 °C (see the Supporting Information for important details regarding the plasma thawing conditions). Experiments with plasma were started within 1 week of thawing. Sodium azide was added to plasma to a final concentration of 0.05% at the beginning of the subunit exchange reaction and after every 10 days during the subunit exchange incubation period. In some experiments, tafamidis (100× stock in DMSO) was added to healthy donor plasma *ex vivo* and the sample was incubated at room temperature for 30 min before being further processed. All samples were centrifuged for 5 min at maximal speed in a tabletop microcentrifuge, and the supernatant was then filtered through a 0.22 μm PVDF filter.

To initiate subunit exchange, FT_2·WT TTR at the indicated concentration was added to the plasma. Unless otherwise indicated, the reaction mixture was incubated at 25 °C for the duration of the subunit exchange period. The subunit exchange reaction can be fit with a single-exponential curve,[23,52,53] consistent with tetramer dissociation being rate-limiting. At each time point of interest during the incubation, 10 μL of the subunit exchange reaction mixture was removed and added to a sample vial containing 3 μL of a 130 μM stock solution of the fluorogenic small molecule **A2** in DMSO.[56] Unless otherwise stated, the samples were incubated with **A2** at 25 °C for 3 h to allow for complete covalent modification by **A2** of the two thyroxine binding sites within the TTR tetramer. After completion of the **A2** conjugation reaction, the sample was diluted by adding 52 μL of 50 μM sodium phosphate buffer (pH 7.6), flash-frozen with liquid nitrogen, and stored at −20 °C for later UPLC analysis. A 50 μL sample was injected onto a

Waters Acquity H-Class Bio-UPLC instrument and eluted as described above for recombinant TTR (see the Supporting Information for details).

Analysis of the Subunit Exchange Reaction. A detailed description of the analysis of the subunit exchange reaction, including the calculation of fraction exchange, is provided in the Results. Rate constants of exchange (k_{ex}) were calculated using GraphPad Prism by plotting the fraction exchange data as a function of time and fitting the results to the first-order single-exponential kinetic equation $y = A(1 - e^{-kt}) + B$. For curves exhibiting very slow kinetics, the plateau value calculated from the single-exponential fit was very different from the theoretical maximum of 1.0 fraction exchange. In these experiments, a constraint was added that the plateau values for all curves within the experiment must be equal, though the precise value was not specified *a priori*. It is also possible to calculate k_{ex} based on the fraction exchange at a single time point using the equation $FE_{t=t} = 1 - e^{-kt}$, which can be solved for $k_{ex,t=t} = -\ln(1 - FE_{t=t})/t$.

Immunoblot Analysis of the UPLC Peaks. Peaks **1**−**5**, corresponding to the five TTR tetramers resulting from subunit exchange, were collected via UPLC after passage through a fluorescence detector. The peak from plasma detected 1−3 min after injection, termed peak **0**, was also collected. Because the concentration of TTR in the collected fractions was predicted to be very low, each peak was collected from four injections of the same sample, pooled, and concentrated using an Amicon Ultra-4 Centrifugal Filter device with a 10 kDa cutoff. The concentrated samples were then volume normalized, analyzed by SDS−PAGE and Western blotting, and detected and quantified using a Li-Cor Odyssey infrared imaging system. Untagged TTR was detected using a polyclonal rabbit anti-TTR antibody (DAKO) at a 1:5000 dilution, and FT_2·WT TTR was detected using the M2 mouse anti-FLAG antibody (Agilent) at a 1:1000 dilution.

HPLC Analysis of Tafamidis Concentrations in Plasma. Frozen plasma samples, collected as described above, were thawed on ice and stored as needed at 4 °C. A standard curve was made for each experiment using plasma from a healthy normal donor and adding 0, 1, 3, 6, 12, or 24 μM tafamidis (final concentration) from 50× stocks in DMSO and then incubating the samples overnight at 37 °C. Plasma was centrifuged for 5 min at maximal speed in a tabletop microcentrifuge. Aliquots of plasma (2 × 20 μL) were mixed with 100 μL of acetonitrile containing 1% (w/v) trichloroacetic acid to precipitate proteins and extract tafamidis. Samples were shaken for 30 min at 25 °C and 1500 rpm and then centrifuged for 10 min at maximal speed in a tabletop microcentrifuge. The supernatant was separated by HPLC using a linear gradient over 20 min (see the Supporting Information for more details). Integration of the tafamidis peak and calculation of the tafamidis concentration using the standard curve were executed in Empower 2 according to the manufacturer's instructions.

RESULTS

Subunit Exchange Rate Differences Reflect TTR Tetramer Kinetic Stability Differences. Co-incubation of equal concentrations of untagged WT TTR and dual-FLAG-tagged WT TTR (FT_2·WT TTR) homotetramers results in subunit exchange between the tetramers.[23,52,53] Subunit exchange is a general property of oligomeric proteins and can be measured using various techniques.[54,57,58] For TTR specifically, under conditions in which TTR aggregation is minimal, such as in plasma where extracellular chaperones like clusterin minimize aggregation,[59,60] the monomeric subunits resulting from tetramer dissociation simply reassemble back to tetramers, a process that is not normally detectable. However, if a population of untagged TTR homotetramers is mixed with a population of tagged homotetramers, the concurrent dissociation of the tagged and untagged tetramers results in a mixed pool of tagged and untagged monomeric TTR subunits (Figure 1A). When these monomers come together during tetramer reassembly, the resulting heterotetramers are made up of tagged and/or untagged TTR subunits (Figure 1A,B). The expected relative area of tetramers **1**−**5** at equilibrium is predicted by a binomial distribution (Figure 1C), where $n = 4$, k is the number of untagged TTR subunits in the peak of interest, and p is the probability of incorporating an untagged TTR subunit, which is the fraction of untagged TTR relative to total TTR, which equals [(area of peak **1** at time zero)/(total area of peaks **1**−**5** at time zero)].

Several lines of evidence indicate that the rate of TTR subunit exchange between WT and FT_2·WT TTR homotetramers is limited by the rate of tetramer dissociation. First, the kinetics of TTR subunit exchange can be rigorously fit to a first-order rate equation, from which a rate constant for subunit exchange, k_{ex}, can be derived. This is true for TTR evaluated over a 200-fold concentration range flanking the physiological range, revealing nearly identical first-order subunit exchange rate constants.[53] The rates at which tetramers **2**−**4** appear and tetramers **1** and **5** disappear are identical within experimental error, consistent with TTR fully dissociating to monomeric subunits before reassembling. If subunit exchange bypassed monomeric intermediates, for example, by proceeding through a dimeric intermediate, the k_{ex} rates for the five tetramers would be expected to differ on the basis of the distribution of the intermediate(s). Second, the rate constant for subunit exchange ($0.027\ h^{-1}$)[53] is very close to the rate constant for tetramer dissociation measured spectroscopically under nonreversible conditions, i.e., between 6 and 8 M urea and extrapolated back to 0 M urea ($0.017\ h^{-1}$).[22] Finally, mathematical modeling of the subunit exchange reaction based on this evidence closely recapitulates the experimental data.[53] Thus, it seems clear that tetramer reassembly is much faster than dissociation,[22,43] that the subunit exchange rate is limited by tetramer dissociation, and that exchange rate differences therefore reflect differences in the kinetic stability of distinct TTR tetramers.

For homotetramer **1** and homotetramer **5**, composed of identical untagged WT and FT_2·WT TTR subunits, respectively, the kinetics of tetramer dissociation and reassociation are identical; thus, the polyanionic dual-FLAG tag does not alter TTR kinetic stability.[52] Heterotetramers comprising untagged WT and FT_2·WT TTR subunits also appear to exhibit identical kinetics of tetramer dissociation and reassociation. Thus, the probability (p) of incorporating an untagged subunit into any tetramer is directly proportional to the relative abundance of untagged TTR. At time zero, the relative abundance of untagged tetramers is represented by the relative area of peak **1** (Figure 1A,B). For each time point, the area of peak **3** is calculated relative to the total area of peaks **1**−**5** (Figure 1C). The fraction exchange at each time point is calculated by dividing the relative area of peak **3** at that time point by the expected relative area of peak **3** at equilibrium, calculated from the binomial distribution (Figure 1C). For example, if the relative area of peak **1** in a given sample at time time zero is 19.22/(19.22 + 1.73 + 12.35) = 0.577, then the expected

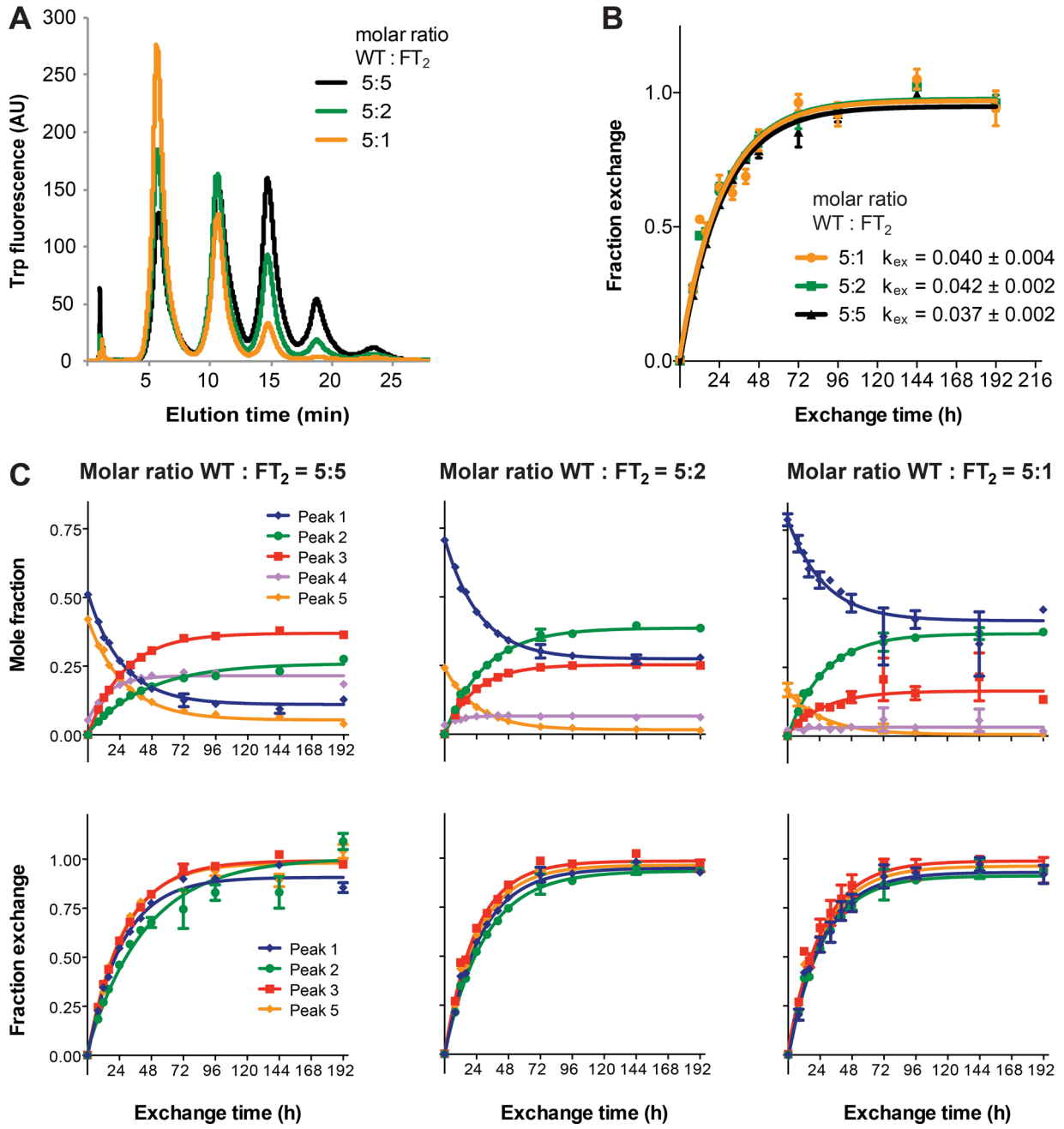

Figure 2. Subunit exchange is a robust measure of TTR tetramer kinetic stability at various ratios of tagged to untagged tetramer concentrations. (A) After incubation in standard phosphate buffer for 8 days, different ratios of the starting concentrations of WT and FT_2·WT TTR yield different ratios of the five tetramer peaks. (B) The kinetics of subunit exchange, as measured by fraction exchange of peak **3**, were followed over a time course of 8 days for the indicated ratios of WT to FT_2·WT TTR. Symbols represent means; error bars represent the SEM, and lines represent fitted curves. (C) The time course of appearance or disappearance of the five tetramer peaks in absolute terms varies according to the molar ratio of the initial populations of WT and FT_2·WT TTR (top panels). However, the time course of the increase in fraction exchange calculated for each peak is very similar (bottom panels): (left) 5 μM WT TTR and 5 μM FT_2·WT TTR, (middle) 5 μM WT TTR and 2 μM FT_2·WT TTR, and (right) 5 μM WT TTR and 1 μM FT_2·WT TTR. Symbols represent means; error bars represent the SEM, and lines represent fitted curves.

relative area of peak **3** at equilibrium is 0.357 based on the binomial distribution. For that same sample, if the relative area of peak **3** after subunit exchange for 7 days is 0.347, then the fraction exchange (FE) will be 0.347/0.357 = 0.97 or 97% (Figure 1C).

All preparations of FT_2·WT TTR homotetramers used for this study contain an impurity that elutes at nearly the same retention time as heterotetramer **4** (Figure 1B) and is likely very similar to heterotetramer **4** (i.e., one of the subunits lacks the N-terminal FT_2 tag). Further purification did not deplete this impurity peak (Figure S1 of the Supporting Information); however, its presence did not meaningfully affect the accuracy of the subunit exchange assay (see the Supporting Information for details). We suspect that this impurity arises from undesirable proteolysis of one subunit within the FT_2·WT TTR homotetramer during biosynthesis in *E. coli*, although we cannot exclude the possibility that it may be some other kind of impurity.

dx.doi.org/10.1021/bi500171j | *Biochemistry* 2014, 53, 1993−2006

Influence of the Concentration of Homotetramers 1 and 5 on TTR Subunit Exchange Kinetics. Previous subunit exchange assays employing recombinant TTR in buffer always maintained equal starting concentrations of WT and FT_2·WT TTR homotetramers. Because endogenous TTR concentrations in plasma vary from patient to patient, we wanted to examine the extent to which varying the starting concentrations of untagged WT and FT_2·WT TTR subunits could influence the kinetics of subunit exchange. We hypothesized that decreasing the starting concentration of homotetramer **5** [FT_2·WT TTR (Figure 1B)] relative to that of homotetramer **1** (untagged WT TTR) would lower the probability of incorporating FT_2·WT TTR subunits into tetramers **2**−**4** during subunit exchange. The recombinant WT TTR homotetramer (5 μM) was incubated with 5, 2, or 1 μM FT_2·WT TTR homotetramer in standard phosphate buffer. Subunit exchange kinetics were followed over the course of 8 days (Figure 2A). As the initial concentrations of WT and FT_2·WT TTR changed, the relative populations of tetramers **1**−**5** at equilibrium changed as expected from the binomial distribution. Importantly, however, the rate of subunit exchange remained constant within error as the concentration of the reporter homotetramer was decreased (Figure 2B). From these results, we conclude that the starting concentration of FT_2·WT TTR relative to that of untagged TTR tetramers does not meaningfully affect the rate of subunit exchange.

To further verify that the kinetics of subunit exchange are invariant to changes in the WT TTR to FT_2·WT TTR relative starting concentrations, we characterized the rate of appearance or disappearance of TTR tetramers **1**−**5** for the indicated starting ratios of WT and FT_2·WT TTR homotetramers (Figure 2C). As expected, the rates of appearance or disappearance of the five peaks in absolute terms (mole fraction) differ as the starting concentrations of WT and FT_2·WT TTR subunits change (Figure 2C, top panels). The equilibrium distribution, calculated using the binomial equation, also changes because it is based on the relative starting concentration of peak **1**. However, the time course of the increase in fraction exchange (Figure 2C, bottom panels) and the calculated subunit exchange rates [k_{ex} (Table 1)] are invariant within error, regardless of the starting ratio of untagged to tagged subunits. At low starting concentrations of FT_2·WT TTR, there is essentially no difference between the area of peak **4** at time zero (impurity peak) and the expected area of peak **4** at equilibrium, and the calculation for fraction exchange based on peak **4** becomes very noisy. Therefore, we have omitted the analysis of peak **4** from the bottom panels in Figure 2C. We conclude that the determination of subunit exchange kinetics is robust when unequal concentrations of tagged and untagged TTR are employed. These results further indicate that the calculation of k_{ex} using peak **3**, used predominantly throughout this work, is representative of the overall subunit exchange rate.

Table 1. Subunit Exchange Rates [k_{ex} (h^{-1})] by Peak for Recombinant TTR in Buffer, at Varying WT:FT_2·WT TTR Molar Ratios[a]

peak	5:5 WT:FT_2·WT TTR molar ratio	5:2 WT:FT_2·WT TTR molar ratio	5:1 WT:FT_2·WT TTR molar ratio
1	0.038 ± 0.001	0.038 ± 0.001	0.037 ± 0.003
2	0.023 ± 0.002	0.033 ± 0.001	0.035 ± 0.001
3	0.037 ± 0.001	0.043 ± 0.002	0.045 ± 0.005
5	0.038 ± 0.002	0.040 ± 0.001	0.040 ± 0.001

[a]Subunit exchange rates (k_{ex}) were calculated from the data presented in Figure 2C.

Detecting Endogenous TTR in Human Plasma Using Fluorogenic Small Molecule A2. Having established that a substoichiometric ratio of FT_2·WT TTR homotetramers (1 μM) to WT TTR homotetramers (5 μM) can be used to quantify TTR subunit exchange in buffer, we next optimized the assay to study TTR subunit exchange in human plasma (in which the TTR tetramer concentration varies from ≈3.4 to 5 μM[19,20]). We wanted to minimize the amount of FT_2·WT TTR added to endogenous TTR in plasma to minimally affect the stoichiometry of tafamidis or diflunisal to the total TTR tetramer concentration in the plasma, to avoid substantially underestimating the extent of TTR kinetic stabilization imparted by a kinetic stabilizer.

The main challenge associated with employing the subunit exchange assay in human plasma is the detection of TTR tetramers over the background of >4000 proteins and additional biomolecules. To facilitate TTR detection in this complex biological fluid, we employed the fluorogenic TTR-modifying small molecule **A2** (Figure 3A).[56] This small molecule rapidly binds to natively folded TTR tetramers, arresting further subunit exchange while remaining non-fluorescent. Only after **A2** chemoselectively acylates the Lys-15 ε-amino group on the periphery of one or both of the thyroxine binding sites does the covalent TTR·**A2** conjugate become fluorescent, allowing specific detection and fluorescence-based quantification of TTR tetramers in plasma. Because the N-terminal dual-FLAG tag does not affect the binding site for **A2**, its use allows for equal fluorescence from all the tetramers comprising recombinant tagged and/or endogenous untagged TTR subunits.

To scrutinize the selectivity of TTR·**A2** conjugate formation in plasma, we started by incubating purified recombinant WT TTR (3 μM) with **A2** (30 μM) in standard phosphate buffer for 3 h before the sample was subjected to anion exchange chromatography by UPLC. The fluorescent conjugate eluted from the column at a retention time of ≈4.5 min (Figure 3A, dotted trace). Incubation of **A2** (30 μM) with human plasma for 3 h revealed a peak at ≈4.25 min (Figure 3A, green trace) as well as an earlier nonretained proteome peak, peak **0**, that eluted between 1 and 3 min (see the Supporting Information for details). No fluorescent peak was detected at 4.25−4.5 min in the plasma of TTR knockout mice (Figure 3A, orange trace) or in human plasma incubated with vehicle lacking **A2** (purple trace). Additional evidence that peak **1** is comprised of endogenous TTR was obtained by immunoblotting, as described below.

We chose to use 30 μM **A2** in our experiments in plasma for two reasons. First, we wanted to allow a conjugate to form with both TTR thyroxine binding pockets in the presence of albumin and other potential binders of **A2** in the complex plasma environment and, later, in the presence of tafamidis. Second, we were confident that this concentration (30 μM) would ensure complete arrest of subunit exchange, as demonstrated below. We found that **A2** fluorescence in plasma is maximal after an incubation period of approximately 2.5 h (Figure 3B) at concentrations exceeding 10 μM (Figure S2A of the Supporting Information), consistent with the reaction kinetics reported previously.[56] The presence of tafamidis (10 μM) does not significantly alter the time course of TTR·**A2** (30

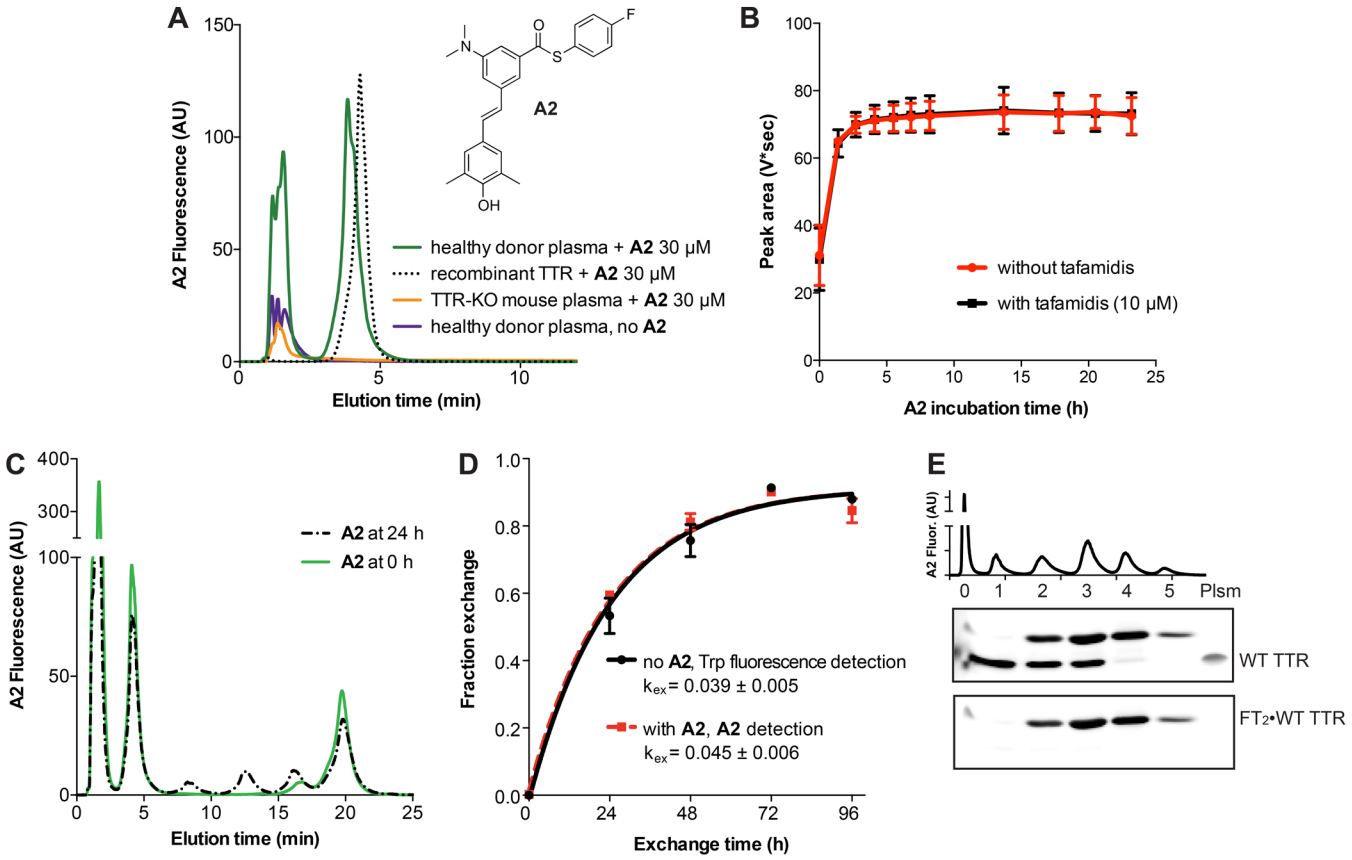

Figure 3. A2 can be used to quantify TTR subunit exchange in blood plasma. (A) Samples were incubated with **A2** or vehicle control for 3 h at 25 °C. The recombinant WT TTR homotetramer peak in standard phosphate buffer (···) is detected at an elution time of 4.5 min. In healthy donor plasma (green line), a similar peak is detected at 4.25 min. This TTR·**A2** conjugate peak is absent in plasma from a TTR knockout (KO) mouse (orange line) and in human plasma that was incubated with vehicle without **A2** (purple line). In all plasma samples, **A2** also detects a peak eluting around 1−3 min (peak **0**). The inset shows the structure of **A2**. (B) Healthy donor plasma was incubated at 25 °C without (red) or with 10 μM tafamidis (black). At time zero, **A2** (30 μM) was added, and the sample was diluted with 5 volumes of sodium phosphate buffer (50 μM, pH 7.6) and immediately placed in the UPLC autosampler to acquire the first time point. Subsequent time points were acquired automatically from the same vial at the indicated times. The area of peak **1** was calculated for each time point. Symbols represent means; error bars represent the SEM. (C) At time zero, 1 μM FT_2·WT TTR was added to healthy donor plasma to initiate the subunit exchange reaction. An aliquot was immediately removed, and **A2** was added at a final concentration of 30 μM (**A2** at 0 h, solid green line). Both samples were incubated at 25 °C for 24 h. At 24 h, a second aliquot was removed and **A2** was added at a final concentration of 30 μM and the mixture incubated at 25 °C for 3 h to allow for complete covalent modification of TTR by **A2** (**A2** at 24 h, dotted black line). Each sample was then analyzed by ion exchange chromatography. (D) Recombinant WT TTR (5 μM) was incubated with FT_2·WT TTR (5 μM) for 96 h. At each time point, subunit exchange was assessed by measuring Trp fluorescence (solid black line) or **A2**·TTR conjugate fluorescence (dotted red line). Symbols represent means; error bars represent the SEM, and lines represent fitted curves. (E) Healthy donor plasma was incubated with FT_2·WT TTR for 21 days. The sample was incubated with **A2** (30 μM) and then separated by ion exchange chromatography (top panel). Peaks were collected from four identical injections, pooled, concentrated, and separated by SDS−PAGE followed by Western blotting for TTR or FLAG-tagged TTR (bottom panels). The expected pattern of WT and FT_2·WT TTR monomers is detected in peaks **1**−**5**. Total human plasma (Plsm) was included as a control.

μM) conjugate formation monitored by fluorescence (Figure 3B), even though **A2** and tafamidis bind to the same thyroxine binding sites in TTR. This result can be explained by the negative cooperativity of binding of tafamidis to the two TTR binding sites: the first binding site in the TTR tetramer is occupied by tafamidis with a higher affinity (k_{d1} = 2 nM) than the second binding site (k_{d2} = 154 nM).[31] At 10 μM tafamidis in plasma, only the first binding site of each TTR tetramer is likely to be occupied.[31] Thus, when one **A2** molecule covalently binds and reacts with TTR, the tafamidis-bound pocket becomes the lower-affinity site, exhibiting a higher rate of tafamidis dissociation, allowing **A2** to bind and react in the second site efficiently. Similar results were obtained when 1 μM FT_2·WT TTR was added to plasma (Figure S2B of the Supporting Information).

As anticipated, we found that addition of **A2** arrests the subunit exchange normally observed between endogenous plasma TTR and FT_2·WT TTR. Following addition of FT_2·WT TTR tetramers (1 μM) to plasma to initiate subunit exchange, an aliquot was immediately removed (time zero) and incubated with **A2** (30 μM) at 25 °C for 24 h. The remainder of the plasma subunit exchange reaction mixture was incubated at 25 °C for 24 h (in the absence of **A2**). At 24 h, a second aliquot from the subunit exchange reaction was removed and added to **A2** (30 μM) for 3 h to allow for complete TTR·**A2** fluorescent conjugate formation. Both aliquots were then fractionated by ion exchange chromatography. The sample in which **A2** was added at time zero showed no subunit exchange during the subsequent 24 h incubation period in the presence of **A2** (Figure 3C). When **A2** was added to an aliquot of the subunit exchange reaction at 24 h, the expected amount of subunit

dx.doi.org/10.1021/bi500171j | *Biochemistry* 2014, 53, 1993−2006

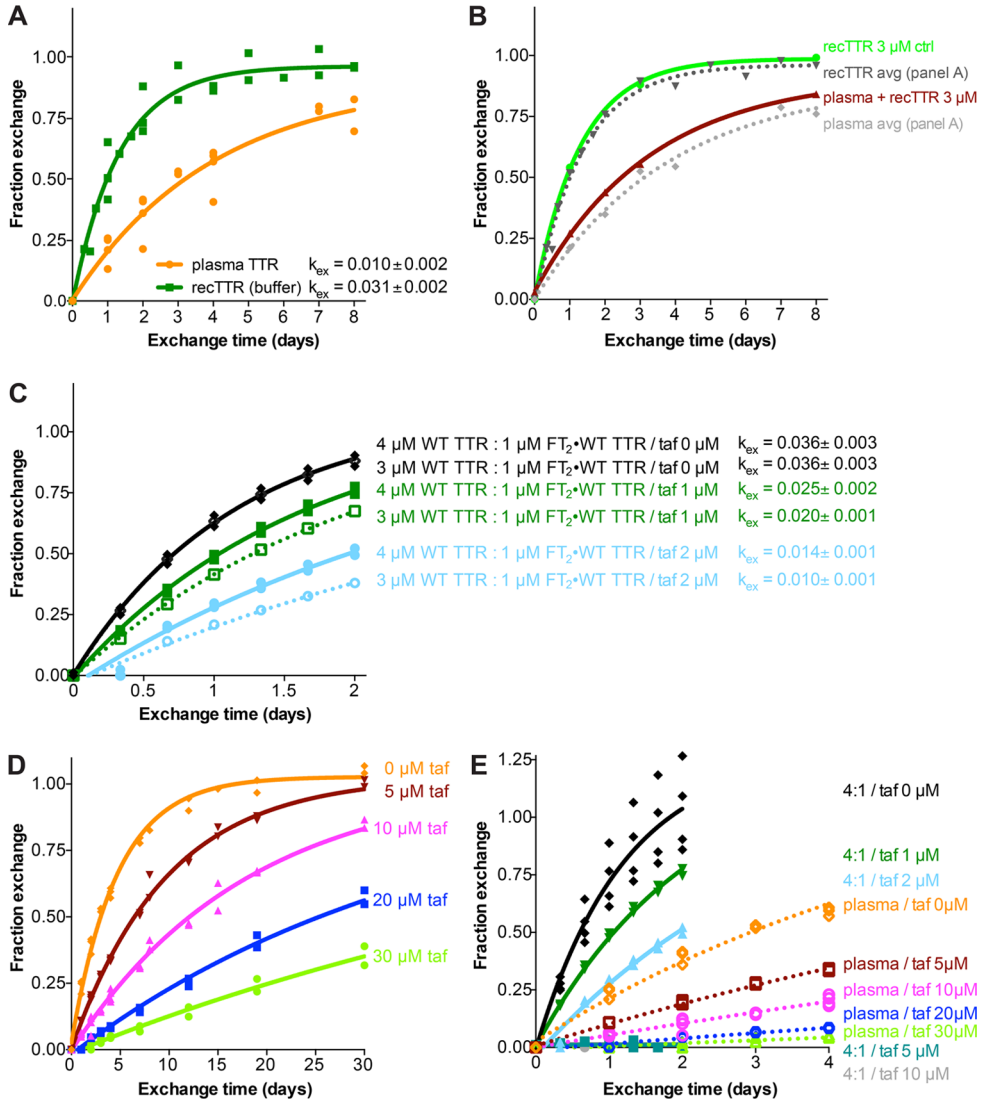

Figure 4. The small molecule tafamidis stabilizes TTR tetramers when added *ex vivo* in human plasma. (A) Subunit exchange was assessed in the presence of 1 μM FT_2·WT TTR in plasma from healthy normal donors (orange) and in standard phosphate buffer containing equal concentrations of recombinant WT and FT_2·WT TTR (green). Symbols represent individual data points; lines represent fitted curves. (B) Recombinant WT TTR (3 μM) was added to endogenous WT TTR (3.8 μM) in a sample of healthy donor plasma (red). FT_2·WT TTR (1 μM) was then added, and subunit exchange was assessed at the indicated time points. Recombinant WT TTR (3 μM) was also incubated with 1 μM FT_2·WT TTR in standard phosphate buffer (green) as a control. The averages of the data for recombinant TTR in standard phosphate buffer (dark gray) and for endogenous TTR in plasma (light gray) from panel A are shown for comparison. Symbols represent individual data points; lines represent fitted curves. (C) Recombinant WT TTR (4 or 3 μM, as indicated) was mixed with FT_2·WT TTR (1 μM) and the indicated concentrations of tafamidis in buffer, and subunit exchange was assessed at the indicated time points. Symbols represent individual data points; lines represent fitted curves. (D) Tafamidis was added *ex vivo* to healthy donor plasma at the indicated concentrations and incubated for 30 min at room temperature. FT_2·WT TTR (1 μM) was then added, and subunit exchange was assessed at the indicated time points. Symbols represent individual data points; lines represent fitted curves. Rate constants and relative fraction exchange were calculated for each condition and are listed in Table 2. (E) Data from panels C and D and Figure S4 of the Supporting Information were graphed on the same set of axes to highlight the difference in the sensitivity of TTR, in buffer and in plasma, to kinetic stabilization by tafamidis.

exchange was observed (Figure 3C). On the basis of these results, we can be confident that no subunit exchange occurs during the 3 h TTR·**A2** fluorescent conjugate formation period used to quantify TTR stabilization in plasma, or in the solutions frozen after the 3 h reaction period with **A2** and awaiting UPLC analysis, ensuring the precision of the collected time points.

Next we probed whether the use of **A2** to render the TTR products of the subunit exchange reaction fluorescent could unexpectedly alter the calculated rate of subunit exchange. To this end, we measured subunit exchange kinetics between recombinant WT and FT_2·WT TTR in standard phosphate buffer, comparing the quantification of the TTR tetramers resulting from subunit exchange using both tryptophan fluorescence-based detection (Figure 3D, black trace) and TTR·**A2** conjugate-based fluorescence detection (Figure 3D, red trace). The calculated rates of exchange from these different detection methods were not significantly different (Figure 3D).

Finally, we show that both endogenous and FT_2·WT TTR can be detected as expected directly in human plasma using TTR·**A2** conjugate-based fluorescence. Plasma was incubated with recombinant FT_2·WT TTR (3 μM) for 21 days, affording an equilibrium distribution of endogenous WT and FT_2·WT

dx.doi.org/10.1021/bi500171j | *Biochemistry* 2014, 53, 1993−2006

TTR heterotetramers. Peaks **1**−**5** were collected from four identical UPLC chromatography runs, pooled, concentrated, and analyzed by SDS−PAGE and immunoblotting, revealing the expected stoichiometry of WT to FT_2·WT TTR in peaks **2**−**4** by gel quantification (Figure 3E).

Because **A2** specifically forms a fluorescent conjugate with folded tetrameric TTR in plasma, the ion exchange chromatograms can be integrated to calculate the concentration of endogenous TTR tetramers in human plasma under native conditions. We generated a standard curve for TTR·**A2** conjugate-based fluorescence using recombinant WT TTR in buffer (Figure S3A of the Supporting Information) and used the resulting calibration line to calculate the concentration of endogenous TTR tetramers in the plasma of a healthy donor, 5.48 μM (Figure S3B of the Supporting Information). We then calculated the concentration of endogenous TTR tetramers in the same plasma sample using quantitative SDS−PAGE immunoblotting (Figure S3C of the Supporting Information) and determined it to be 5.48 μM. Therefore, we conclude that the integration of the TTR·**A2** conjugate-based fluorescence chromatograms at time zero in the subunit exchange reaction can be used to rigorously quantify the endogenous TTR tetramer concentration in human plasma. Because **A2** labels only natively folded TTR tetramers, whereas SDS−PAGE denatures all TTR conformations to the component denatured monomers, we conclude that essentially all of the TTR in this healthy donor plasma is natively folded.

Subunit Exchange of Endogenous TTR in Plasma Is Slower Than Exchange of Recombinant TTR in Buffer. It is clear that WT TTR subunit exchange is slower in plasma than it is in buffer. It takes 22.0 h to achieve 50% subunit exchange in buffer, whereas it takes 66.5 h to achieve 50% exchange in plasma (Figure 4A). Further analysis showed that the rate of exchange in plasma was approximately 3-fold slower than that in buffer. Preliminary data indicate that the higher stability of TTR tetramers in plasma is not sufficiently explained by molecular crowding, as crowding only modestly stabilizes TTR. This interesting, previously unreported effect is apparently due to a molecule present in plasma, as adding recombinant WT TTR (3 μM) to the plasma of a healthy donor causes recombinant TTR to adopt the exchange rate of endogenous plasma TTR (Figure 4B). We are aggressively pursuing an explanation, which will be reported in due time.

Pharmacologic TTR Kinetic Stabilization *ex Vivo* Can Be Quantified by Subunit Exchange. Tafamidis is a TTR kinetic stabilizer with demonstrated efficacy in slowing the progression of FAP, as shown by clinical trial data and a 12 month extension study.[9,10] To date, the effects of tafamidis on TTR subunit exchange have been measured only in buffer, and only using equal concentrations of tagged and untagged recombinant TTR.[31] TTR kinetic stabilization by tafamidis is known to be sensitive to the stoichiometry of tafamidis to total TTR tetramer concentration.[31] Therefore, we hypothesized that the degree of stabilization measured by subunit exchange in plasma from tafamidis-treated patients could be sensitive to the variations in the concentration of endogenous TTR across individuals, and that it would be important to minimize the amount of recombinant FT_2·WT TTR added to the plasma for the same reasons.

We first tested this hypothesis using recombinant TTR in buffer. To simulate the differences between individual plasma samples, we added 1 μM FT_2·WT TTR to either 3 or 4 μM recombinant WT TTR. Various concentrations of tafamidis were then added to these samples, and subunit exchange was followed over a time course of 48 h. As expected, in the absence of tafamidis, the concentration of WT relative to FT_2·WT TTR concentration (1 μM) had no effect on the subunit exchange rate (Figure 4C). However, in the presence of tafamidis, differences in the WT TTR concentration relative to the FT_2·WT TTR concentration (1 μM) were reflected in the subunit exchange rate (Figure 4C). These anticipated differences in subunit exchange rates are due to differences in the stoichiometry of tafamidis to total TTR tetramer concentration. For example, adding 2 μM tafamidis to the samples with 3 μM WT TTR and 1 μM FT_2·WT TTR yields a tafamidis:total TTR tetramer ratio of 1:2. However, adding 2 μM tafamidis to the samples with 4 μM WT TTR and 1 μM FT_2·WT TTR leads to a tafamidis:total TTR tetramer ratio of 1:2.5. When tafamidis was added at a concentration of 5 or 10 μM to these samples (tafamidis:TTR tetramer ratio of $\geq$1.0), subunit exchange was arrested during the time course of the experiment (Figure S4 of the Supporting Information). These experiments show that although variability in the ratio of WT to FT_2·WT TTR does not affect the subunit exchange rate in the absence of tafamidis, small changes in the stoichiometry of tafamidis relative to the total tetrameric TTR concentration, as might occur in individual patients, do affect the observed rate of subunit exchange, as expected. Because the use of **A2** allows for precise quantification of the endogenous TTR concentration in each plasma sample at the start of all subunit exchange experiments, these differences can be integrated into subsequent analyses of subunit exchange rates.

Next, we quantified the kinetic stabilization of endogenous TTR directly in human plasma by adding tafamidis at various concentrations *ex vivo* to the plasma of healthy donors. A fixed amount of recombinant FT_2·WT TTR (1 μM) was then added, and the stability of the endogenous TTR tetramers was measured by subunit exchange. Using standard curves for TTR·**A2** conjugate fluorescence like those shown in Figure S3 of the Supporting Information, we calculated that the concentration of TTR tetramers in the plasma of these donors was 3.1 ± 0.6 μM. We found that tafamidis increased TTR kinetic stability in a dose-dependent manner in plasma, yielding decreases of 52, 74, 87, and 93% at tafamidis plasma concentrations of 5, 10, 20, and 30 μM, respectively (Figure 4D and Table 2). It is important to be mindful of the 48 h half-life of TTR in human plasma when interpreting these data, as there is very little tetramer dissociation over this period when tafamdis is present

Table 2. Effects of Incubation of Tafamidis *ex Vivo* on Subunit Exchange Kinetic Parameters in Human Plasma[a]

[tafamidis] (μM)	k_{ex} (h^{-1})	SE k_{ex}[b]	$t_{1/2}$[c] (days)	change in k_{ex}[d] (%)
0[e]	8.91×10^{-3}	2.93×10^{-4}	3.24	−
5	4.29×10^{-3}	1.23×10^{-4}	6.73	−51.8
10	2.31×10^{-3}	6.37×10^{-5}	12.52	−74.1
20	1.12×10^{-3}	4.12×10^{-5}	25.71	−87.4
30	5.98×10^{-4}	3.10×10^{-5}	48.31	−93.3

[a]Subunit exchange rates and half-times, as well as the change in subunit exchange rates relative to vehicle control, were calculated from the data presented in Figure 4D. [b]SE k_{ex} is the standard error of k_{ex}. [c]$t_{1/2}$ is the time needed for the subunit exchange reaction to reach a fraction exchange of 0.5. [d]The change in k_{ex} is calculated relative to the vehicle control as $[(k_{ex}$ of interest$) - (k_{ex}$ of vehicle$)]/(k_{ex}$ of vehicle$) \times 100$. [e]The DMSO vehicle control is 0 μM tafamidis.

dx.doi.org/10.1021/bi500171j | *Biochemistry* 2014, 53, 1993−2006

at plasma concentrations from 10 to 20 μM, which can be achieved with 20 mg oral dosing once daily (see below).

The TTR subunit exchange rate in buffer is more responsive to changes in tafamidis concentration than is the exchange rate in plasma (Figure 4E). This observation was expected because in plasma, tafamidis can also bind to other proteins, including albumin. For example, it is known that tafamidis added to plasma *ex vivo* at a concentration of 7.2 μM binds the two available TTR binding pockets with a stoichiometry of 0.81 tafamidis molecule per TTR tetramer.[31]

Although subunit exchange can be monitored for up to 30 days, as in Figure 4D, we reiterate that the half-life of endogenous TTR in plasma is approximately 2 days.[61,62] Therefore, the biological significance of differences in the kinetic stability of TTR tetramers should be interpreted from experiments on the time scale of 2−4 days. All experiments described in the following sections were followed over a time course of 8 days, but we have focused our quantification and interpretation on the 48 and 96 h time points for this reason.

The Temperature Dependence of Subunit Exchange Is Attenuated by Tafamidis-Mediated Kinetic Stabilization. Previous work showed that recombinant TTR in buffer exchanges subunits on a time scale of hours at 4 °C and on a time scale of days at 37 °C.[52] The results presented thus far are from subunit exchange reactions conducted at 25 °C. This temperature was chosen as a compromise because 25 °C is more physiologically relevant than 4 °C[35,52,63] and at 25 °C subunit exchange is fast enough to be convenient on a laboratory time scale. However, we wanted to be certain that experiments conducted at 25 °C provide a reasonable approximation of the more physiologically relevant subunit exchange reactions that occur at 37 °C. Thus, we investigated the effect of temperature on the subunit exchange rate exhibited by endogenous TTR in plasma and on the kinetic stabilization of endogenous TTR resulting from *ex vivo* addition of tafamidis. In the absence of tafamidis, endogenous TTR in plasma exchanged subunits at 25 °C 3.6-fold faster than at 37 °C. Surprisingly, the temperature-dependent differences in kinetic stability, as discerned by subunit exchange, were markedly attenuated in the presence of tafamidis at all concentrations tested (Figure 5A,B). Thus, for example, the rate of exchange in the presence of 10 μM tafamidis was only 2.6-fold faster at 25 °C than at 37 °C. We conclude that subunit exchange experiments conducted at 25 °C do reflect tafamidis-associated stabilization nicely but suggest that studies for selecting doses of tafamidis for various TTR genotypes should be conducted at 37 °C to ensure that such critical patient-centered decisions are based on the most physiologically relevant data possible.

Pharmacologic TTR Kinetic Stabilization in Patient Plasma Can Be Quantified by Subunit Exchange. To demonstrate that the subunit exchange assay can be used to quantify the kinetic stability of endogenous TTR in patients taking tafamidis orally (20 mg once daily), senile systemic amyloidosis (SSA) patients who were orally treated with tafamidis for months leading up to this study were compared to untreated SSA patients and untreated age-matched controls. Subunit exchange was followed over 8 days (Figure S5 of the Supporting Information). Because the half-life of endogenous TTR in plasma is approximately 2 days,[61,62] we chose to focus on the 48 and 96 h time points. As expected, the fraction exchange at 48 h (Figure 6A) was lower than the fraction exchange at 96 h (Figure 6B) for each sample. It is interesting

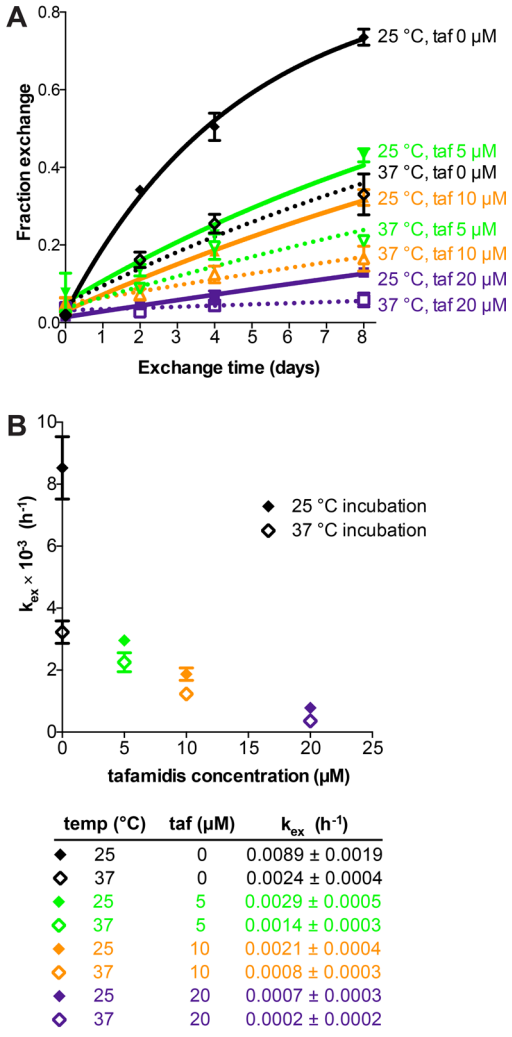

temp (°C)	taf (μM)	k_{ex} (h^{-1})
25	0	0.0089 ± 0.0019
37	0	0.0024 ± 0.0004
25	5	0.0029 ± 0.0005
37	5	0.0014 ± 0.0003
25	10	0.0021 ± 0.0004
37	10	0.0008 ± 0.0003
25	20	0.0007 ± 0.0003
37	20	0.0002 ± 0.0002

Figure 5. Sensitivity of TTR subunit exchange to incubation temperature is attenuated by tafamidis stabilization. Tafamidis was added at the indicated concentrations to plasma from three healthy donors and incubated for 30 min at room temperature. Each sample was then split into two aliquots for incubation at 25 or 37 °C. FT_2·WT TTR (1 μM) was added to each aliquot. (A) Subunit exchange was assessed at the indicated time points over a time course of 8 days. Filled symbols and solid lines represent data from 25 °C; empty symbols and dotted lines represent data from 37 °C. Symbols represent means; error bars represent the SEM, and lines represent fitted curves. (B) The rate of tetramer dissociation (k_{ex}) was calculated for each sample using a least-squares fit to a one-phase association model in GraphPad Prism. Filled symbols represent data from 25 °C; empty symbols represent data from 37 °C, and error bars represent the SEM.

to note that there was less variability within each group at 48 h exchange, suggesting that this time point is optimal for maximizing the signal-to-noise ratio of the subunit exchange assay and reflects the half-life of TTR in humans. The rate of tetramer dissociation (subunit exchange rate, k_{ex}) was calculated for each individual from the 48 and 96 h time points separately and plotted on one set of axes (Figure 6C) as filled ($k_{ex,48\ h}$) and empty symbols ($k_{ex,96\ h}$), where each individual is represented by a distinct color. The stability of endogenous TTR in the plasma of untreated SSA patients was not significantly different from that of the age-matched controls. In contrast, the TTR in tafamidis-treated SSA patients

dx.doi.org/10.1021/bi500171j | *Biochemistry* 2014, 53, 1993−2006

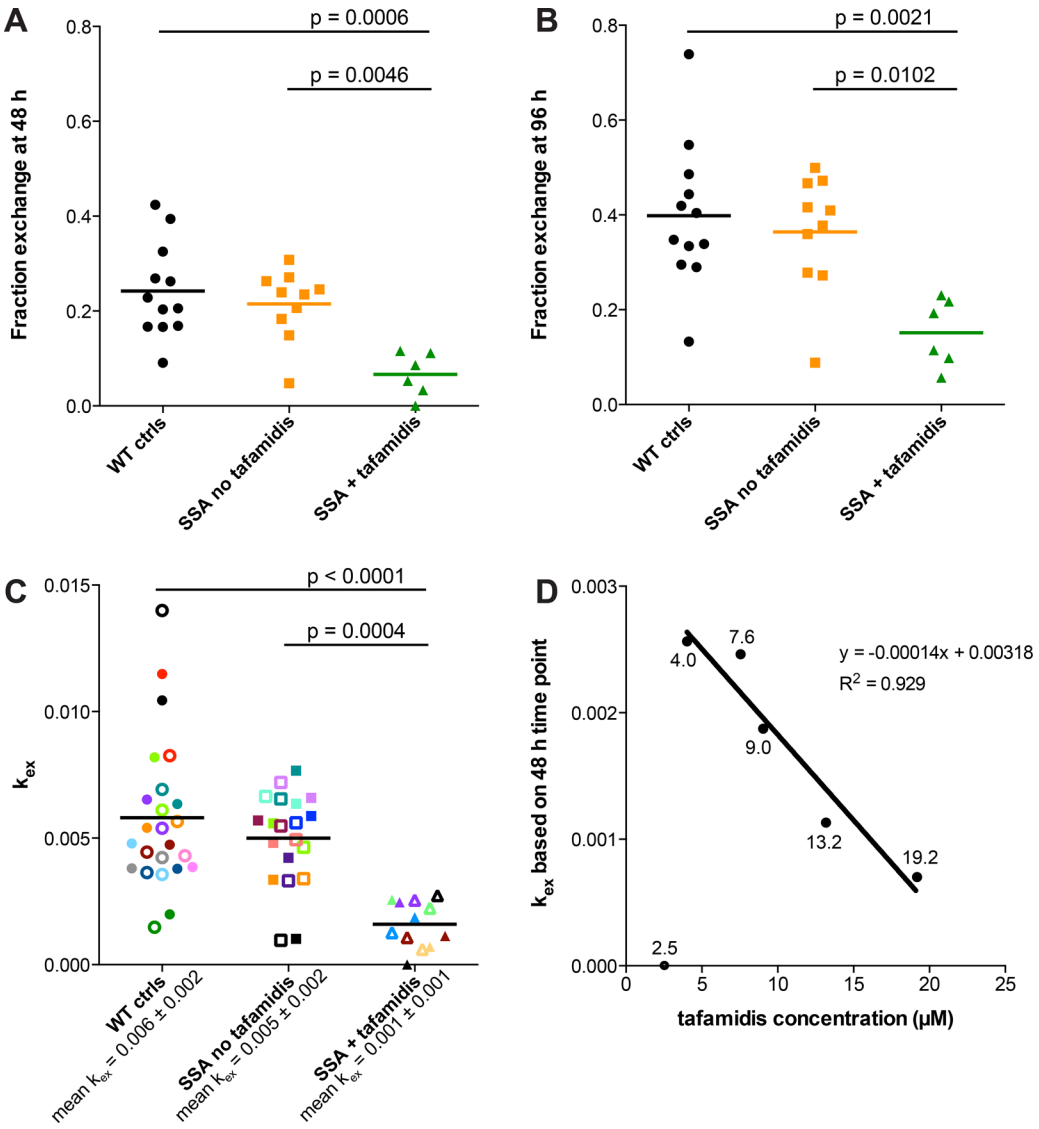

Figure 6. TTR kinetic stabilization by orally administered tafamidis can be measured directly in patient plasma. (A and B) Plasma samples were obtained from SSA patients treated with 20 mg of tafamidis once daily (SSA + tafamidis, green triangles), SSA patients not treated with tafamidis (SSA no tafamidis, orange squares), and age-matched controls (WT ctrls, black circles). For each sample, subunit exchange was quantified at 48 (A) and 96 h (B), and fraction exchange was calculated as described. Differences between groups were assessed by one-way analysis of variance (ANOVA) followed by Tukey's post hoc test. (C) The rate of tetramer dissociation (k_{ex}) was calculated for each sample from each time point using the equation $k_{ex,t=t} = -\ln(1 - FE_{t=t})/t$. The k_{ex} values calculated from the 48 h subunit exchange incubation (filled symbols) and from the 96 h subunit exchange incubation (empty symbols) were plotted on the same set of axes, with each individual patient represented by a different color. Differences between groups were assessed by one-way ANOVA followed by Tukey's post hoc test. (D) The k_{ex} values calculated from the 48 h subunit exchange data were plotted as a function of the concentration of tafamidis measured in each sample by HPLC. The data (excluding the outlier with a calculated k_{ex} of 0) were fit by a linear regression model, yielding a calibration line with the equation $y = -0.00014x + 0.00318$ (R^2 = 0.929).

exhibited a >73% decrease in the tetramer dissociation rate (Figure 6C).

Finally, we investigated the extent to which tetramer stabilization in each patient, as measured by subunit exchange at 48 h, correlates with the concentration of the kinetic stabilizer tafamidis in a patient's blood. Tafamidis levels in the plasma from the six tafamidis-treated SSA patients were quantified by HPLC. Excluding one outlier whose calculated k_{ex} at 48 h was 0, we found the rate of tetramer dissociation (subunit exchange) correlated strongly with tafamidis concentration in the plasma (Figure 6D; R^2 = 0.929). Stabilization of TTR by tafamidis has been shown to lead to modest increases in the plasma concentration of TTR itself.[9,10] However, we did not detect a correlation between the rate of tetramer dissociation (subunit exchange rate) and TTR tetramer concentration as calculated from TTR·**A2** conjugate fluorescence (Figure S6 of the Supporting Information). While these preliminary results are exciting, further work with greater numbers of individuals is needed to confirm and expand on these findings.

DISCUSSION

Herein, we describe a subunit exchange assay that facilitates quantification of endogenous TTR kinetic stability in human blood plasma in the presence of all of the factors, both established and unknown, which may contribute to the kinetic

dx.doi.org/10.1021/bi500171j | *Biochemistry* 2014, 53, 1993−2006

stability of this protein. Central to the utility of this method is the small amount of the recombinant FT_2·WT TTR (1 μM) reporter tetramer that is added to plasma. The fluorogenic native TTR tetramer probe **A2**, which reacts with and renders the TTR tetramers in the plasma fluorescent, also plays a critical role in that it allows ion exchange chromatography to be conducted on the plasma proteome, resolving peaks **1**−**5** and thus allowing subunit exchange to be quantified.

In addition, the subunit exchange assay in patient plasma allows the direct quantification of the stability imparted by oral tafamidis administration. Tafamidis is a kinetic stabilizer that slows the progression of FAP, one of the TTR amyloid diseases. While 90% of V30M FAP patients taking tafamidis progress at less than one-fifth of the rate of untreated patients,[9,10] it is not currently known why 10% of the treated population progresses faster. Many factors could contribute, including differences in TTR post-translational modifications, compliance issues, variance in the absorption/metabolism of tafamidis, or variations in the levels of endogenous small molecule TTR binders or binding proteins that contribute to TTR stability in plasma. Indeed, our results show that there is some variability in the degree of stabilization of plasma TTR from different individuals, even in the presence of identical doses of tafamidis delivered *ex vivo* (Figure 4D). These findings underscore the need for a personalized, quantitative measure of TTR stabilization to ensure optimal tafamidis dosing for each patient. The subunit exchange method for quantifying TTR stability in human plasma enables such personalized medicine. In addition, ongoing studies on the correlations between the kinetic stabilization of TTR afforded by tafamidis treatment and clinical outcomes have the potential to shed more light on the physiopathology of the TTR amyloidoses.

An accurate measurement of TTR kinetic stability is also critical for optimal treatment of the familial TTR amyloidoses as a function of genotype. Different mutations in the *TTR* sequence often alter the binding constants of the kinetic stabilizer to the TTR tetramers, necessitating personalized treatment regimens. We envision that this quantification method can be helpful in the case of rare disease-associated mutations, allowing clinicians to choose the appropriate dose of drug for optimal or maximal TTR stabilization, as clinical trials or even clinical studies may not be practical for these small populations.

Several of the findings reported herein were unexpected. The 3.1-fold slower exchange of plasma TTR, compared with that of recombinant human TTR in buffer (Figure 4A), indicates that a molecule(s) in plasma stabilizes TTR tetramers in a way that has not previously been appreciated. Therefore, experiments using recombinant protein probably overestimate TTR's aggregation propensity in the body. We speculate that holo-retinol binding protein,[64] an endogenous small molecule, protein, or some combination of factors kinetically stabilizes endogenous TTR in plasma relative to recombinant TTR in buffer. We are aggressively seeking a molecular explanation for these differences. As expected, tafamidis-associated kinetic stabilization of TTR in buffer is more effective than kinetic stabilization in plasma at identical concentrations of tafamidis (Figure 4E), likely because of nonspecific binding of tafamidis to other proteins in plasma such as albumin. This observation highlights the importance of assessing TTR kinetic stability under native conditions, i.e., in the presence of all potential interactors in plasma. Differences in the rate of tetramer dissociation (subunit exchange) as a function of temperature were expected, but we were surprised to find that these differences are attenuated in the presence of tafamidis (Figure 5B). While the level of TTR stabilization at a given tafamidis concentration is greater in buffer, endogenous TTR in plasma is inherently more kinetically stable; thus, dose suitability assessments are best conducted in patient plasma at 37 °C.

The subunit exchange assay was employed herein to quantify the stabilization of TTR from senile systemic amyloidosis patients being chronically treated with tafamidis (20 mg orally, once daily). The significant TTR kinetic stability imparted by oral tafamidis dosing correlated strongly with the tafamidis plasma concentrations, suggesting the possible utility of this method as a surrogate biomarker.

In summary, we believe that the subunit exchange assay, either alone or in combination with another methodology, could be useful in establishing the optimal dose of kinetic stabilizer for individual patients, for quantifying the response to tafamidis treatment, and possibly for use as a biomarker for early diagnosis. Upon correlation of tafamidis-associated kinetic stabilization of TTR with clinical outcomes of patients treated with tafamidis, the subunit exchange assay could become a surrogate biomarker likely to predict clinical outcomes in this population.

■ ASSOCIATED CONTENT

Supporting Information

Supporting methods and Figures S1−S6. This material is available free of charge via the Internet at http://pubs.acs.org.

■ AUTHOR INFORMATION

Corresponding Author

*E-mail: jkelly@scripps.edu. Phone: (858) 784-9880.

Author Contributions

I.R. and C.M. contributed equally to this work.

Funding

This work was supported by National Institutes of Health Grant DK046335 (J.W.K.) as well as the Skaggs Institute for Chemical Biology and the Lita Annenberg Hazen Foundation. I.R. was supported by a National Research Service Award fellowship from the National Institute of General Medical Sciences (F32-GM099364).

Notes

The authors declare the following competing financial interest(s): J.W.K. discovered tafamidis and benefits from its sale.

■ ACKNOWLEDGMENTS

We thank Dr. Joseph Genereux for helpful discussions, Dr. Colleen Fearns for critical reading of the manuscript, and Michael Saure and Gina Dendle for technical support.

■ ABBREVIATIONS

FAP, familial amyloid polyneuropathy; FE, fraction exchange; FT_2·WT TTR, dual FLAG-tagged wild-type TTR; SDS−PAGE, sodium dodecyl sulfate−polyacrylamide gel electrophoresis; SEM, standard error of the mean; SSA, senile systemic amyloidosis; TTR, transthyretin; UPLC, ultra performance liquid chromatography; WT, wild type.

■ REFERENCES

(1) Merlini, G., and Bellotti, V. (2003) Molecular mechanisms of amyloidosis. *N. Engl. J. Med. 349*, 583−596.

(2) Morten, I. J., Hewitt, E. W., and Radford, S. E. (2007) β2-microglobulin and dialysis-related amyloidosis. *Protein Rev. 6*, 217−239 (213 plates).
(3) Foguel, D., and Silva, J. L. (2004) New Insights into the Mechanisms of Protein Misfolding and Aggregation in Amyloidogenic Diseases Derived from Pressure Studies. *Biochemistry 43*, 11361−11370.
(4) Cao, P., Marek, P., Noor, H., Patsalo, V., Tu, L.-H., Wang, H., Abedini, A., and Raleigh, D. P. (2013) Islet amyloid: From fundamental biophysics to mechanisms of cytotoxicity. *FEBS Lett. 587*, 1106−1118.
(5) Chiti, F., and Dobson, C. M. (2006) Protein misfolding, functional amyloid, and human disease. *Annu. Rev. Biochem. 75*, 333−366.
(6) Kelly, J. W. (1998) The alternative conformations of amyloidogenic proteins and their multi-step assembly pathways. *Curr. Opin. Struct. Biol. 8*, 101−106.
(7) Givens, R. C., Russo, C., Green, P., and Maurer, M. S. (2013) Comparison of cardiac amyloidosis due to wild-type and V122I transthyretin in older adults referred to an academic medical center. *Aging Health 9*, 229−235.
(8) Westermark, P., Sletten, K., Johansson, B., and Cornwell, G. G., III (1990) Fibril in senile systemic amyloidosis is derived from normal transthyretin. *Proc. Natl. Acad. Sci. U.S.A. 87*, 2843−2845.
(9) Coelho, T., Maia, L. F., da Silva, A. M., Cruz, M. W., Plante-Bordeneuve, V., Suhr, O. B., Conceicao, I., Schmidt, H. H., Trigo, P., Kelly, J. W., Labaudiniere, R., Chan, J., Packman, J., and Grogan, D. R. (2013) Long-term effects of tafamidis for the treatment of transthyretin familial amyloid polyneuropathy. *J. Neurol. 260*, 2802−2814.
(10) Coelho, T., Maia, L. F., Martins, d. S. A., Waddington, C. M., Plante-Bordeneuve, V., Lozeron, P., Suhr, O. B., Campistol, J. M., Conceicao, I. M., Schmidt, H. H. J., Trigo, P., Kelly, J. W., Labaudiniere, R., Chan, J., Packman, J., Wilson, A., Grogan, D. R., Imventarza, O. C., Wainberg, P. J., Berra, L. M., Maultasch, H., Gold, J., Bardera, J. C. P., and Zibert, A. (2012) Tafamidis for transthyretin familial amyloid polyneuropathy: A randomized, controlled trial. *Neurology 79*, 785−792.
(11) Berk, J. L., Suhr, O. B., Obici, L., Sekijima, Y., Zeldenrust, S. R., Yamashita, T., Hennegan, M. A., Gorevic, P. D., Litchy, W. J., Wiseman, J. F., Nordh, E., Corato, M., Lozza, A., Cortese, A., Robinson-Papp, J., Colton, T., Rybin, D. V., Bisbee, A. B., Ando, Y., Ikeda, S., Seldin, D. C., Merlini, G., Skinner, M., Kelly, J. W., and Dyck, P. J. (2013) Repurposing Diflunisal for Familial Amyloid Polyneuropathy: A Randomized Clinical Trial. *JAMA, J. Am. Med. Assoc. 310*, 2658−2667.
(12) Colon, W., and Kelly, J. W. (1992) Partial denaturation of transthyretin is sufficient for amyloid fibril formation in vitro. *Biochemistry 31*, 8654−8660.
(13) Carulla, N., Zhou, M., Giralt, E., Robinson, C. V., and Dobson, C. M. (2010) Structure and intermolecular dynamics of aggregates populated during amyloid fibril formation studied by hydrogen/deuterium exchange. *Acc. Chem. Res. 43*, 1072−1079.
(14) Booth, D. R., Sunde, M., Bellotti, V., Robinson, C. V., Hutchinson, W. L., Fraser, P. E., Hawkins, P. N., Dobson, C. M., Radford, S. E., Blake, C. C., and Pepys, M. B. (1997) Instability, unfolding and aggregation of human lysozyme variants underlying amyloid fibrillogenesis. *Nature 385*, 787−793.
(15) Hurle, M. R., Helms, L. R., Li, L., Chan, W., and Wetzel, R. (1994) A role for destabilizing amino acid replacements in light-chain amyloidosis. *Proc. Natl. Acad. Sci. U.S.A. 91*, 5446−5450.
(16) Monaco, H. L., Rizzi, M., and Coda, A. (1995) Structure of a complex of two plasma proteins: Transthyretin and retinol-binding protein. *Science 268*, 1039−1041.
(17) Blake, C. C., Geisow, M. J., Oatley, S. J., Rerat, B., and Rerat, C. (1978) Structure of prealbumin: Secondary, tertiary and quaternary interactions determined by Fourier refinement at 1.8 Å. *J. Mol. Biol. 121*, 339−356.
(18) Schreiber, G., and Richardson, S. J. (1997) The evolution of gene expression, structure and function of transthyretin. *Comp. Biochem. Physiol., Part B: Biochem. Mol. Biol. 116*, 137−160.
(19) Audet-Delage, Y., Ouellet, N., Dallaire, R., Dewailly, E., and Ayotte, P. (2013) Persistent organic pollutants and transthyretin-bound thyroxin in plasma of Inuit women of childbearing age. *Environ. Sci. Technol. 47*, 13086−13092.
(20) Henze, A., Espe, K. M., Wanner, C., Krane, V., Raila, J., Hocher, B., Schweigert, F. J., and Drechsler, C. (2012) Transthyretin predicts cardiovascular outcome in hemodialysis patients with type 2 diabetes. *Diabetes Care 35*, 2365−2372.
(21) Hurshman, A. R., White, J. T., Powers, E. T., and Kelly, J. W. (2004) Transthyretin aggregation under partially denaturing conditions is a downhill polymerization. *Biochemistry 43*, 7365−7381.
(22) Hammarstrom, P., Jiang, X., Hurshman, A. R., Powers, E. T., and Kelly, J. W. (2002) Sequence-dependent denaturation energetics: A major determinant in amyloid disease diversity. *Proc. Natl. Acad. Sci. U.S.A. 99* (Suppl. 4), 16427−16432.
(23) Hammarstrom, P., Wiseman, R. L., Powers, E. T., and Kelly, J. W. (2003) Prevention of transthyretin amyloid disease by changing protein misfolding energetics. *Science 299*, 713−716.
(24) Hurshman Babbes, A. R., Powers, E. T., and Kelly, J. W. (2008) Quantification of the thermodynamically linked quaternary and tertiary structural stabilities of transthyretin and its disease-associated variants: The relationship between stability and amyloidosis. *Biochemistry 47*, 6969−6984.
(25) Foss, T. R., Kelker, M. S., Wiseman, R. L., Wilson, I. A., and Kelly, J. W. (2005) Kinetic stabilization of the native state by protein engineering: Implications for inhibition of transthyretin amyloidogenesis. *J. Mol. Biol. 347*, 841−854.
(26) Foss, T. R., Wiseman, R. L., and Kelly, J. W. (2005) The pathway by which the tetrameric protein transthyretin dissociates. *Biochemistry 44*, 15525−15533.
(27) Jiang, X., Buxbaum, J. N., and Kelly, J. W. (2001) The V122I cardiomyopathy variant of transthyretin increases the velocity of rate-limiting tetramer dissociation, resulting in accelerated amyloidosis. *Proc. Natl. Acad. Sci. U.S.A. 98*, 14943−14948.
(28) Lashuel, H. A., Wurth, C., Woo, L., and Kelly, J. W. (1999) The most pathogenic transthyretin variant, L55P, forms amyloid fibrils under acidic conditions and protofilaments under physiological conditions. *Biochemistry 38*, 13560−13573.
(29) Jiang, X., Smith, C. S., Petrassi, H. M., Hammarstrom, P., White, J. T., Sacchettini, J. C., and Kelly, J. W. (2001) An engineered transthyretin monomer that is nonamyloidogenic, unless it is partially denatured. *Biochemistry 40*, 11442−11452.
(30) Lai, Z., Colon, W., and Kelly, J. W. (1996) The acid-mediated denaturation pathway of transthyretin yields a conformational intermediate that can self-assemble into amyloid. *Biochemistry 35*, 6470−6482.
(31) Bulawa, C. E., Connelly, S., DeVit, M., Wang, L., Weigel, C., Fleming, J. A., Packman, J., Powers, E. T., Wiseman, R. L., Foss, T. R., Wilson, I. A., Kelly, J. W., and Labaudiniere, R. (2012) Tafamidis, a potent and selective transthyretin kinetic stabilizer that inhibits the amyloid cascade. *Proc. Natl. Acad. Sci. U.S.A. 109*, 9629−9634.
(32) Andrade, C. (1952) A peculiar form of peripheral neuropathy; familiar atypical generalized amyloidosis with special involvement of the peripheral nerves. *Brain 75*, 408−427.
(33) Coelho, T. (1996) Familial amyloid polyneuropathy: New developments in genetics and treatment. *Curr. Opin. Neurol. 9*, 355−359.
(34) Coelho, T., Chorao, R., Sousa, A., Alves, I., Torres, M. F., and Saraiva, M. J. (1996) Compound heterozygotes of transthyretin Met30 and transthyretin Met119 are protected from the devastating effects of familial amyloid polyneuropathy. *Neuromuscular Disord. 6*, 27.
(35) Hammarstrom, P., Schneider, F., and Kelly, J. W. (2001) Trans-suppression of misfolding in an amyloid disease. *Science 293*, 2459−2462.
(36) Johnson, S. M., Connelly, S., Fearns, C., Powers, E. T., and Kelly, J. W. (2012) The Transthyretin Amyloidoses: From Delineating

the Molecular Mechanism of Aggregation Linked to Pathology to a Regulatory-Agency-Approved Drug. *J. Mol. Biol. 421*, 185−203.
(37) Hornstrup, L. S., Frikke-Schmidt, R., Nordestgaard, B. G., and Tybjaerg-Hansen, A. (2013) Genetic stabilization of transthyretin, cerebrovascular disease, and life expectancy. *Arterioscler., Thromb., Vasc. Biol. 33*, 1441−1447.
(38) Benson, M. D. (1989) Familial Amyloidotic Polyneuropathy. *Trends Biochem. Sci. 12*, 88−92.
(39) Falk, R. H. (2011) Cardiac amyloidosis: A treatable disease, often overlooked. *Circulation 124*, 1079−1085.
(40) Connors, L. H., Richardson, A. M., Theberge, R., and Costello, C. E. (2000) Tabulation of transthyretin (TTR) variants as of 1/1/2000. *Amyloid 7*, 54−69.
(41) Connors, L. H., Lim, A., Prokaeva, T., Roskens, V. A., and Costello, C. E. (2003) Tabulation of human transthyretin (TTR) variants, 2003. *Amyloid. 10*, 160−184.
(42) McCutchen, S. L., Lai, Z., Miroy, G. J., Kelly, J. W., and Colon, W. (1995) Comparison of lethal and nonlethal transthyretin variants and their relationship to amyloid disease. *Biochemistry 34*, 13527−13536.
(43) Sekijima, Y., Wiseman, R. L., Matteson, J., Hammarstrom, P., Miller, S. R., Sawkar, A. R., Balch, W. E., and Kelly, J. W. (2005) The biological and chemical basis for tissue-selective amyloid disease. *Cell 121*, 73−85.
(44) Nettleton, E. J., Sunde, M., Lai, Z., Kelly, J. W., Dobson, C. M., and Robinson, C. V. (1998) Protein subunit interactions and structural integrity of amyloidogenic transthyretins: Evidence from electrospray mass spectrometry. *J. Mol. Biol. 281*, 553−564.
(45) Razavi, H., Palaninathan, S. K., Powers, E. T., Wiseman, R. L., Purkey, H. E., Mohamedmohaideen, N. N., Deechongkit, S., Chiang, K. P., Dendle, M. T., Sacchettini, J. C., and Kelly, J. W. (2003) Benzoxazoles as transthyretin amyloid fibril inhibitors: Synthesis, evaluation, and mechanism of action. *Angew. Chem. 42*, 2758−2761.
(46) Baures, P. W., Peterson, S. A., and Kelly, J. W. (1998) Discovering transthyretin amyloid fibril inhibitors by limited screening. *Bioorg. Med. Chem. 6*, 1389−1401.
(47) Sekijima, Y., Dendle, M. A., and Kelly, J. W. (2006) Orally administered diflunisal stabilizes transthyretin against dissociation required for amyloidogenesis. *Amyloid 13*, 236−249.
(48) Miller, S. R., Sekijima, Y., and Kelly, J. W. (2004) Native state stabilization by NSAIDs inhibits transthyretin amyloidogenesis from the most common familial disease variants. *Lab. Invest. 84*, 545−552.
(49) Dyck, P. J., Albers, J. W., Andersen, H., Arezzo, J. C., Biessels, G.-J., Bril, V., Feldman, E. L., Litchy, W. J., O'Brien, P. C., and Russell, J. W. (2011) Diabetic Polyneuropathies: Update on Research Definition, Diagnostic Criteria and Estimation of Severity. *Diabetes/Metab. Res. Rev. 27*, 620−628.
(50) Coelho, T., Carvalho, M., Saraiva, M. J., Alves, I., Almeida, M. R., and Costa, P. P. (1993) A strikingly benign evolution of FAP in an individual found to be a compound heterozygote for two TTR mutations: TTR MET 30 and TTR MET 119. *J. Rheumatol. 20*, 179.
(51) Palhano, F. L., Leme, L. P., Busnardo, R. G., and Foguel, D. (2009) Trapping the monomer of a non-amyloidogenic variant of transthyretin: Exploring its possible use as a therapeutic strategy against transthyretin amyloidogenic diseases. *J. Biol. Chem. 284*, 1443−1453.
(52) Schneider, F., Hammarstrom, P., and Kelly, J. W. (2001) Transthyretin slowly exchanges subunits under physiological conditions: A convenient chromatographic method to study subunit exchange in oligomeric proteins. *Protein Sci. 10*, 1606−1613.
(53) Wiseman, R. L., Green, N. S., and Kelly, J. W. (2005) Kinetic stabilization of an oligomeric protein under physiological conditions demonstrated by a lack of subunit exchange: Implications for transthyretin amyloidosis. *Biochemistry 44*, 9265−9274.
(54) Keetch, C. A., Bromley, E. H., McCammon, M. G., Wang, N., Christodoulou, J., and Robinson, C. V. (2005) L55P transthyretin accelerates subunit exchange and leads to rapid formation of hybrid tetramers. *J. Biol. Chem. 280*, 41667−41674.
(55) McCammon, M. G., Scott, D. J., Keetch, C. A., Greene, L. H., Purkey, H. E., Petrassi, H. M., Kelly, J. W., and Robinson, C. V. (2002) Screening transthyretin amyloid fibril inhibitors: Characterization of novel multiprotein, multiligand complexes by mass spectrometry. *Structure 10*, 851−863.
(56) Choi, S., Ong, D. S., and Kelly, J. W. (2010) A stilbene that binds selectively to transthyretin in cells and remains dark until it undergoes a chemoselective reaction to create a bright blue fluorescent conjugate. *J. Am. Chem. Soc. 132*, 16043−16051.
(57) Raju, I., Oonthonpan, L., and Abraham, E. C. (2012) Mutations in human αA-crystallin/sHSP affect subunit exchange interaction with αB-crystallin. *PLoS One 7*, e31421.
(58) Kallur, L. S., Aziz, A., and Abraham, E. C. (2008) C-Terminal truncation affects subunit exchange of human αA-crystallin with αB-crystallin. *Mol. Cell. Biochem. 308*, 85−91.
(59) Poon, S., Treweek, T. M., Wilson, M. R., Easterbrook-Smith, S. B., and Carver, J. A. (2002) Clusterin is an extracellular chaperone that specifically interacts with slowly aggregating proteins on their off-folding pathway. *FEBS Lett. 513*, 259−266.
(60) Humphreys, D. T., Carver, J. A., Easterbrook-Smith, S. B., and Wilson, M. R. (1999) Clusterin has chaperone-like activity similar to that of small heat shock proteins. *J. Biol. Chem. 274*, 6875−6881.
(61) Socolow, E. L., Woeber, K. A., Purdy, R. H., Holloway, M. T., and Ingbar, S. H. (1965) Preparation of I-131-labeled human serum prealbumin and its metabolism in normal and sick patients. *J. Clin. Invest. 44*, 1600−1609.
(62) Oppehneimer, J. H., Surks, M. I., Bernstein, G., and Smity, J. C. (1965) Metabolism of Iodine-131-Labeled Thyroxine-Binding Prealbumin in Man. *Science 149*, 748−750.
(63) Hammarstrom, P., Jiang, X., Deechongkit, S., and Kelly, J. W. (2001) Anion shielding of electrostatic repulsions in transthyretin modulates stability and amyloidosis: Insight into the chaotrope unfolding dichotomy. *Biochemistry 40*, 11453−11459.
(64) Hyung, S. J., Deroo, S., and Robinson, C. V. (2010) Retinol and retinol-binding protein stabilize transthyretin via formation of retinol transport complex. *ACS Chem. Biol. 5*, 1137−1146.